



**University of
Zurich^{UZH}**

**Zurich Open Repository and
Archive**

University of Zurich
University Library
Strickhofstrasse 39
CH-8057 Zurich
www.zora.uzh.ch

Year: 2012

**Tissue engineered bone grafts based on biomimetic nanocomposite
PLGA/amorphous calcium phosphate scaffold and human adipose-derived
stem cells**

Buschmann, Johanna ; Härter, Luc ; Gao, Shuping ; Hemmi, Sonja ; Welti, Manfred ; Hild, Nora ;
Schneider, Oliver D ; Stark, Wendelin J ; Lindenblatt, Nicole ; Werner, Clement M L ; Wanner, Guido
A ; Calcagni, Maurizio

Abstract: For tissue engineering of critical size bone grafts, nanocomposites are getting more and more attractive due to their controllable physical and biological properties. We report in vitro and in vivo behaviour of an electrospun nanocomposite based on poly-lactic-co-glycolic acid and amorphous calcium phosphate nanoparticles (PLGA/a-CaP) seeded with human adipose-derived stem cells (ASC) compared to PLGA. Major findings were that cell attachment, three-dimensional ingrowth and proliferation were very good on both materials. Cell morphology changed from a spindle-shaped fibroblast-like form to a more roundish type when ASC were seeded on PLGA, while they retained their morphology on PLGA/a-CaP. Moreover, we found ASC differentiation to a phenotype committed towards osteogenesis when a-CaP nanoparticles were suspended in normal culture medium without any osteogenic supplements, which renders a-CaP nanoparticles an interesting osteoinductive component for the synthesis of other nanocomposites than PLGA/a-CaP. Finally, electrospun PLGA/a-CaP scaffold architecture is suitable for a rapid and homogenous vascularisation confirmed by a complete penetration by avian vessels from the chick chorioallantoic membrane (CAM) within one week.

DOI: <https://doi.org/10.1016/j.injury.2012.06.004>

Posted at the Zurich Open Repository and Archive, University of Zurich

ZORA URL: <https://doi.org/10.5167/uzh-73067>

Journal Article

Accepted Version

Originally published at:

Buschmann, Johanna; Härter, Luc; Gao, Shuping; Hemmi, Sonja; Welti, Manfred; Hild, Nora; Schneider, Oliver D; Stark, Wendelin J; Lindenblatt, Nicole; Werner, Clement M L; Wanner, Guido A; Calcagni, Maurizio (2012). Tissue engineered bone grafts based on biomimetic nanocomposite PLGA/amorphous calcium phosphate scaffold and human adipose-derived stem cells. *Injury*, 43(10):1689-1697.

DOI: <https://doi.org/10.1016/j.injury.2012.06.004>

Tissue engineered bone grafts based on biomimetic nanocomposite PLGA/amorphous calcium phosphate scaffold and human adipose-derived stem cells[☆]

Johanna Buschmann^{a,d,*}, Luc Härter^{b,d}, Shuping Gao^b, Sonja Hemmi^b, Manfred Welti^a, Nora Hild^c, Oliver D. Schneider^c, Wendelin J. Stark^c, Nicole Lindenblatt^a, Clement M.L. Werner^b, Guido A. Wanner^b, Maurizio Calcagni^a

^a Division of Plastic and Hand Surgery, University Hospital Zurich, ZKF, Sternwartstrasse 14, CH-8091 Zurich, Switzerland

^b Division of Trauma Surgery, University Hospital Zurich, ZKF, Sternwartstrasse 14, CH-8091 Zurich, Switzerland

^c Institute for Chemical and Bioengineering, Department of Chemistry and Applied Biosciences, ETH Zurich, CH-8093 Zurich, Switzerland

ARTICLE INFO

Article history:
Accepted 1 June 2012

Keywords:
Electrospinning
Nanocomposite
Nanoparticles
PLGA
Amorphous calcium phosphate
Bone graft
ASC

ABSTRACT

For tissue engineering of critical size bone grafts, nanocomposites are getting more and more attractive due to their controllable physical and biological properties. We report *in vitro* and *in vivo* behaviour of an electrospun nanocomposite based on poly lactic co glycolic acid and amorphous calcium phosphate nanoparticles (PLGA/a CaP) seeded with human adipose derived stem cells (ASC) compared to PLGA. Major findings were that cell attachment, three dimensional ingrowth and proliferation were very good on both materials. Cell morphology changed from a spindle shaped fibroblast like form to a more roundish type when ASC were seeded on PLGA, while they retained their morphology on PLGA/a CaP. Moreover, we found ASC differentiation to a phenotype committed towards osteogenesis when a CaP nanoparticles were suspended in normal culture medium without any osteogenic supplements, which renders a CaP nanoparticles an interesting osteoinductive component for the synthesis of other nanocomposites than PLGA/a CaP. Finally, electrospun PLGA/a CaP scaffold architecture is suitable for a rapid and homogenous vascularisation confirmed by a complete penetration by avian vessels from the chick chorioallantoic membrane (CAM) within one week.

© 2012 Published by Elsevier Ltd.

Introduction

Nanocomposites such as poly (lactic co glycolide)/amorphous nano calcium phosphate (PLGA/a CaP) offer an exciting approach to combine the advantages of a biocompatible and degradable polymer and a mineral component in order to optimize the physical and biological properties of a scaffold material aimed at bone reconstruction.^{1–4} Natural bone primarily consists of a nano structured composite of hydroxyapatite and collagen.⁵ Artificial graft materials have been synthesized to mimic bone matrix, ranging from different pure calcium phosphate compounds,⁶ biphasic calcium phosphate,⁷ β TCP ceramics^{8,9} to combinations of organic and inorganic components such as PLGA/nano hydroxyapatite,¹⁰

PLGA/ β TCP,¹¹ collagen/nano hydroxyapatite¹² or pure organic polymers, for example DegraPol^{®13} or PLGA.¹⁴

Strategies in bone reconstruction are diverse.¹⁵ Besides the relevant choice of a suitable scaffold material, different approaches have been developed to overcome the main bottleneck for critical size bone grafts, namely an insufficient supply of oxygen and nutrients to the middle of the graft ending up in a necrotic central core. With this regard, the supply of vasculogenic cells in combination with either osteoblasts or with stem cells seems to be promising.^{16–19} Other methods involve cell and gene therapy, for example with marrow derived stromal cells expressing VEGF in a controlled way,⁴ *in situ* preformed vessels to allow rapid anastomosis²⁰ or creation of an artero venous loop based on the local conductance of the host vessels.²¹ Muller et al. claim, however, that even with the highest loaded (stem) cell densities and independent of the scaffold material used, frank bone generation critically needs osteoblasts or in the case of stem cells an osteogenic commitment of those cells. This commitment is either achieved by pre differentiation *in vitro*, a low dose of osteogenic factors or by orthotopic environmental conditions.²²

[☆] The work was performed at the University Hospital Zurich, ZKF, Sternwartstrasse 14, 8091 Zurich, Switzerland.

* Corresponding author. Tel.: +41 44 255 98 95.

E-mail address: johanna.buschmann@usz.ch (J. Buschmann).

^d These authors contributed equally to this work.

In the study presented here, we chose an electrospun nanocomposite PLGA/a CaP as a scaffold material,² which has been shown to give promising results when applied as such (no cell seeding) for non critical size calvarial defects in rabbit and sheep models.^{23,24} Because adipose derived stem cells (ASC) have been shown to be easily extracted from fat tissue and to give high yields compared to bone marrow derived stem cells,^{25,26} we chose human ASC for seeding the nanocomposite PLGA/a CaP. The aims of this study were (i) to assess the suitability of electrospun PLGA/a CaP nanocomposites seeded with human ASC as a tissue engineered graft for bone reconstruction (control neat (pure) PLGA scaffold), (ii) to evaluate the trigger function of a CaP nanoparticles for the differentiation of ASC into cells of the osteoblast lineage and (iii) to test whether the electrospun PLGA/a CaP scaffold is vascularised homogenously after ectopic implantation on the chick chorioallantoic membrane (CAM) assay.

60 Materials and methods

61 Scaffolds

Two different scaffold materials were used. Clinically approved PLGA (85:15) was received from Boehringer Ingelheim. The a CaP nanoparticles (Ca/P = 1.5) were prepared by flame spray pyrolysis as described by Lohr et al.²⁷ using calcium 2 ethyl hexanoic salt (synthesized by calcium hydroxide from Riedel de Haen, Ph. Eur. and ethylhexanoic acid from Sigma Aldrich) and tributyl phosphate (98% Sigma Aldrich). Amorphous calcium phosphate nanoparticles (PLGA/a CaP) was prepared according to.² To combine the two components, the a CaP nanoparticles were dispersed in chloroform (Riedel de Haen, Ph. Eur.) containing 5 wt% (referring to the later on added polymer) Tween20 (Polysorbate20, Fluka, Ph. Eur.) using an ultrasonic bath (Bandelin Sonorex Digitec). PLGA (8 wt% in chloroform) was added to the dispersion (PLGA/a CaP = 60/40 wt) and the mixture was stirred at room temperature overnight. Pure PLGA solutions (prepared without corresponding amount of nanoparticles) and the PLGA/a CaP dispersions were electrospun (feeding rate: 2 mL/h; distance tip collector: 10 cm; voltage applied: 20 kV for PLGA/a CaP and 4 mL/h, 20 cm, 20 kV, respectively, for pure PLGA; tip kept in a chloroform airstream).² The surface of the as prepared scaffolds was investigated by means of scanning electron microscopy Transmission electron microscopy (TEM, FEI, Philips CM 12) was used to obtain particle morphology and to determine the particles' primary diameter (~22 nm). SEM and TEM images of these materials are shown in Fig. 1.

Disks of 1 cm in diameter and ~200 µm in height were prepared of PLGA and of PLGA/a CaP, while tubes with a length of 2 cm, an inner diameter of 2 mm and a wall thickness of ~800 µm were prepared based on electrospun PLGA/a CaP scaffolds. For the CAM assay (see below), the tubes were cut into four equal pieces of 0.5 cm length. All scaffolds were sterilised with ethylenoxide for 4.5 h at 37 °C before use.

94 Cell cultures and flow cytometry

ASC were isolated from abdominal fat tissue with the consent of the patient (female, 45 years, no pathology) according to Swiss (KEK ZH: StV 7 2009) and international ethical guidelines (ClinicalTrials.gov Identifier: NCT01218945). The extraction procedure is referenced in.^{28,29} Cells were cultivated to confluency in αMEM medium supplemented with 10% foetal bovine serum (FBS) (Biowest, Teco Medical, Sissach, Switzerland), 1 ng mL⁻¹ β FGF and 50 µg mL⁻¹ gentamycine (Biowest, Teco Medical, Sissach, Switzerland). For the experiments, cells were cultured in DMEM medium (Biowest, Teco Medical, Sissach, Switzerland),

complemented by 10% of FBS and 50 µg mL⁻¹ gentamycine. Cell counting was done with the Neubauer chamber (n = 4). Only passages 4, 5 and 7 (P4, P5 and P7) were used for all experiments.

Lineage specific differentiation of ASC towards the chondrogenic, the osteogenic, the adipogenic and the endothelial cell lineage was achieved with media supplementation according to Zuk et al.²⁸. ASC phenotyping was characterized according to established procedures.³⁰ For flow cytometric analyses (FACS), ASC were harvested using trypsin EDTA digestion, and resuspended in PBS (2 × 10⁶ mL⁻¹). Aliquots of ASC (1 × 10⁵) were stained for 30 min at room temperature (RT) with respective monoclonal antibody solution (diluted 1:25), subsequently fixed with para formaldehyde (0.1% final) for 30 min at RT and FACS. Primary antibodies labelled with phycoerythrin (PE) were CD13 PE (Becton Dickinson), unlabeled were CD29 (sc 59828, Santa Cruz), CD44 (sc 59758, Santa Cruz), CD105 (sc 18838, Santa Cruz), CD34 (sc 19621, Santa Cruz), CD31 (sc 53411, Santa Cruz), CD146 (sc 18837, Santa Cruz) and osteocalcin (sc 73464, Santa Cruz). Unlabeled antibodies were detected using a respective secondary antibody (Goat anti mouse IgG PE, Santa Cruz, USA). In this case, ASC were washed once in PBS after primary staining and then incubated with the PE labelled secondary antibody (diluted 1:25) for 30 min at RT. Phycoerythrin fluorescence of individual cells was measured with a FACSCalibur flow cytometer (Becton Dickinson AG, Basel, Switzerland), gating on physical parameters to exclude cell debris. A minimum of 10,000 events per gate were counted per sample.

Human osteoblasts (OB) were isolated from a male trauma patient (age 26 years; providing informed consent) undergoing osteosynthesis with bone grafting from the iliac crest and cultured in α MEM medium (Biowest, Teco Medical, Sissach, Switzerland), complemented by 20% of FBS and 50 µg mL⁻¹ gentamycine.³¹ Passage 2 was used as a primary reference cell line.

3D cultures on the scaffolds

The PLGA disks, the PLGA/a CaP disks and the PLGA/a CaP tubes were soaked in 10 mL DMEM medium with 10% of FBS and 50 µg mL⁻¹ gentamycine for 15 min and dried in the laminar flow bench. For the disks, 5 × 10⁵ ASC from either P4 or P7 in 100 µL cell culture medium were seeded on top of the disc and absorbed by the material. For the tubes, 10⁶ ASC in 150 µL cell culture medium were seeded outside and 10⁶ ASC were seeded inside the tube. The cell distribution outside was constant over the whole length of the tube, while it was restricted inside the tube to the middle part by inert plastic tips of about 1 cm length put on both sides. Such conic plastic tips were needed to avoid the leakage of the cells before proper attachment. The tips were removed the day after seeding. Without any lag time between cell seeding and immersion into the medium, all seeded scaffolds were cultivated in 6 well plates using 7 mL DMEM medium with 10% of FBS and 50 µg mL⁻¹ gentamycine for 1 and 2 weeks, respectively, in a humidified atmosphere of 95% air and 5% CO₂ at 37 °C. Medium was changed every 3 or 4 days. The samples were fixed overnight by 4% formalin in PBS (Kantonsapotheke Zurich, Switzerland) and stained afterwards. Sample size was n = 4.

Experiments with a CaP nanoparticles

To 5 × 10⁵ ASC (P4) in a chamber slide (DMEM culture medium with 10% of FBS, 200 µg mL⁻¹ gentamycine and 2.5 µg mL⁻¹ amphotericine B) freshly diluted a CaP nanoparticles DMEM suspensions (sonicated) were added with different final concentrations, namely 5, 50 and 500 µg mL⁻¹, respectively. An ASC culture without nanoparticles served as negative control. After 1 and 2 weeks the cultures were analyzed by immunofluorescence

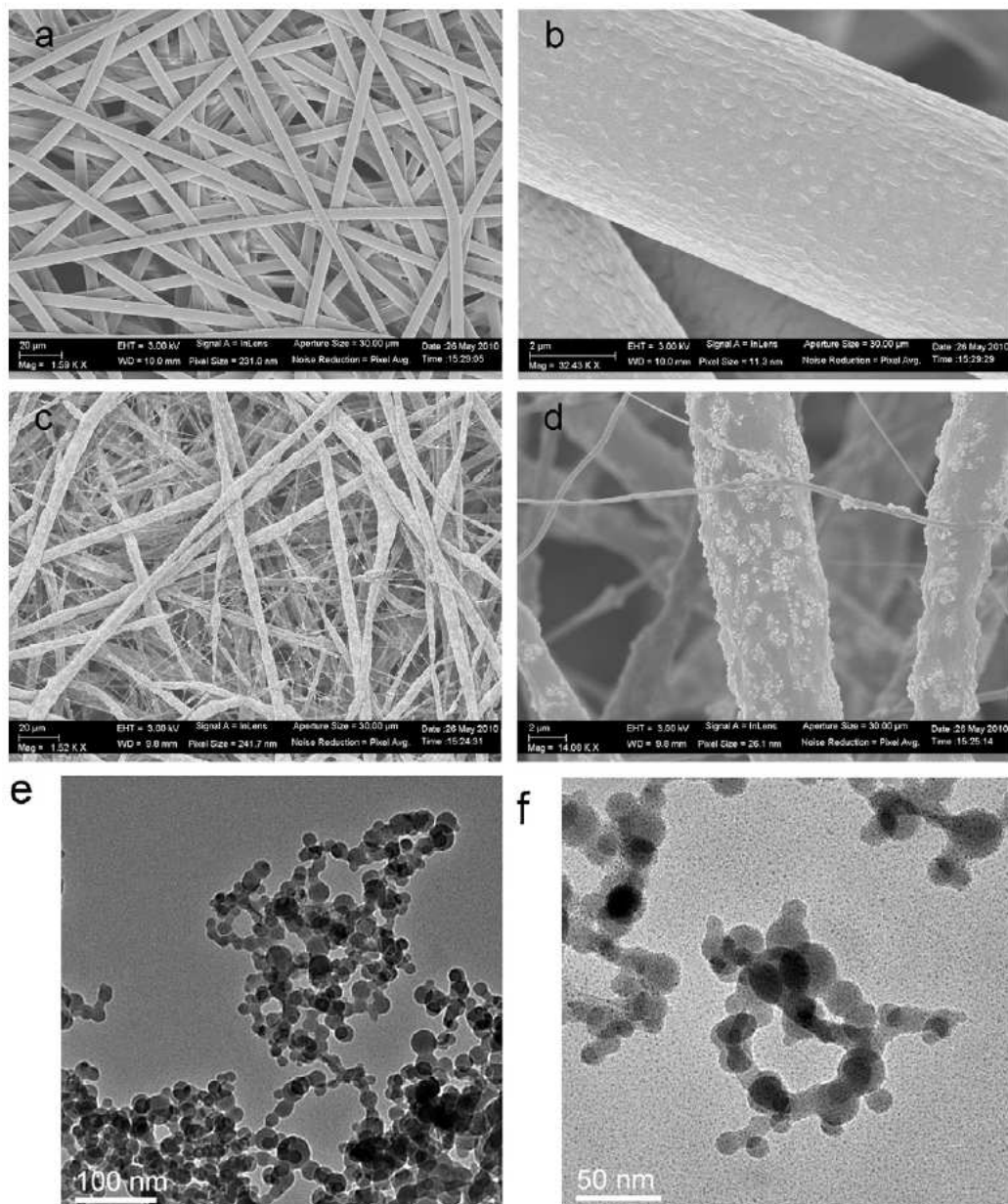


Fig. 1. SEM images of electrospun PLGA (a and b) and PLGA/a-CaP (c and d). TEM images of a-CaP nanoparticles (e and f).

for osteocalcin (FITC, green). Briefly, cells were fixed by cold methanol (4 °C), flushed with DPBS, incubated firstly with 0.15% saponin (Fluka, Switzer) and 0.1% bovine serum albumine (BSA) (Fluka, Switzerland) and secondly with 0.50% saponin and 0.1% BSA for 15 min. The first antibody, rabbit anti human osteocalcin (MorphoSys AbD GmbH, Düsseldorf, number 7060 1525 7E), was applied overnight at 4 °C (diluted 1:30). After washing with DPBS, the second antibody, goat anti rabbit FITC (Reactolab S. A., Servion, Switzerland, number DI 1488F) was applied in a 1:150 dilution in the dark. After a washing step, DAPI was applied for 5 min at RT in order to visualize the cell nuclei (blue). The human OB primary cells (P2) served as a positive control. Sample size was $n = 3$ for all conditions.

Chick chorioallantoic membrane (CAM) assay: implantation of scaffolds onto the CAM

Fertilized Lowman white LSL chick eggs (Animalco AG Geflügelzucht, Hermenweg 21, 5603 Staufen, Switzerland) were

incubated at 37 °C and 65% relative humidity (constant during the whole experiment) for 3.5 days. Then, the egg shell was removed and the embryo and all remaining parts were carefully placed into an O₂ permeable plastic bowl (6 cm in diameter, No 710.0, Thermoflex, Switzerland) (*ex ovo* technique). The eggs were incubated for another 4.5 days. At incubation day (ID) 8, the PLGA disks, the PLGA/a CaP disks as well as the PLGA/a CaP tubes (0.5 cm in length) were carefully put on top of the CAM. Afterwards, the CAM assays were reincubated for 7 days until ID 15. Afterwards, the CAM was fixated overnight by a 4% formalin solution in PBS (Kantonsapotheke Zurich, Switzerland). Finally, the scaffolds were removed by cutting (*ex vivo* samples), and the scaffolds were embedded in paraffin. Sample size was $n = 3$.

Histological analyses

After deparaffinizing with xylene and rehydrating the 7 µm paraffin sections (descending gradient of ethanol), they were differently stained:

- (a) by Haematoxylin Eosin (H&E) staining in order to show the erythrocytes (dark pink), other cells (blue) and collagenous tissue (light violet),
- (b) by Sudan, Hemalaun (analogously to Haematoxylin Eosin (H&E) staining, with replacement of the eosin by Sudan red) in order to show the PLGA (light red), cells (pale blue) and the extracellular matrix (brownish),
- (c) by Masson Goldner Trichrome in order to show erythrocytes and endothelial cells (dark red), cell nuclei (black) for detection of mitosis and collagenous tissue (green).
- (d) Alizarin Red staining in order to visualize bone like calcium depositions.

The cell width of ASC on either PLGA or PLGA/a CaP material was determined in the Hemalaun/Sudan stained histological sections at a 400× magnification with a light microscope (Leica DM 6000 B) equipped with a digital camera. For ASC on PLGA 70 fields of view (FOV) were analyzed and for PLGA/a CaP 80 FOV were analyzed.

Extracellular matrix (ECM) production was evaluated in the Masson Goldner Trichrome stained sections as the percentage of the whole scaffold area in 16 FOV of PLGA and 16 FOV of PLGA/a CaP at 200× magnification using *analysis^D* software.

Statistics

The data were analyzed with StatView 5.0.1. Statistical analysis of variance (ANOVA) was conducted to test the significance of differences between different time points (1 week versus 2 weeks) used for the quantification of ASC numbers on PLGA/a CaP tubes, for the ASC width as well as the ECM production on different scaffold materials. Pairwise comparison probabilities (*p*) were calculated using the Fisher's PLSD and the Bonferroni post hoc test. *P* values <0.05 were considered significant. Values were expressed as means ± standard deviations if not otherwise stated.

Results

Characterization of ASC

Cultured in flasks under normal conditions ASC exhibited a spindle shaped and fibroblast like morphology, this was also seen when ASC were cultivated in DMEM. Analysis of surface antigens by FACS demonstrated that typical stem cell markers such as CD13, CD29, CD44 and CD105 were expressed with high MFI, while CD31, CD34 and CD146 had low MFI (Table 1 and Supplementary information, Fig. S1). In addition, ASC were able to undergo osteogenic (Osteocalcin, Alizarin Red staining), chondrogenic (morphology, Alcian Blue staining), endothelial differentiation (CD31, CD34) and adipogenic differentiation (Oil Red O) (data not shown).

Behaviour of ASC on PLGA and on PLGA/a CaP

In order to evaluate the impact of a CaP nanoparticles bound to a PLGA scaffold on the cultivation and growth of seeded ASC, we compared ASC cultivation on PLGA disks with PLGA/a CaP disks (paraffin sections). The three dimensional ingrowth of ASC into the scaffold material was good for both materials, with a 200 µm thick disc being homogenously penetrated by ASC after 1 week (Fig. 2). Cell mitosis as detected in histological staining inside the scaffold was qualitatively found for both materials (Fig. 2a and b).

In contrast, the cell morphology of ASC proliferating on PLGA was different compared to ASC on PLGA/a CaP. Whereas the ASC seeded on PLGA/a CaP retained their morphology, namely a spindle shaped and fibroblast like form, the ASC seeded on PLGA

Table 1

FACS analysis. Relative intensities of MFI of P1 to P4 for the ASC extracted from abdominal fat (0 low intensity and +++ high intensity).

	MFI (P1)	MFI (P2)	MFI (P3)	MFI (P4)
CD13	+++	+++	+++	+++
CD29	+++	+++	+++	+++
CD44	++	+	+	++
CD105	++	++	++	+
CD31	0	0	0	+
CD34	0	0	0	+
CD146	0	0	0	+

turned rather roundish during the incubation period (Fig. 2c and d). The width of the cells were found to be significantly different with $4.6 \pm 1.7 \mu\text{m}$ ($n = 70$) for ASC on PLGA and $3.5 \pm 1.7 \mu\text{m}$ ($n = 80$) for ASC on PLGA/a CaP after one week with $p < 0.0001$ (Bonferroni post hoc test; Fig. 2e). In addition, extracellular matrix (ECM) production was found to be advanced with the PLGA/a CaP material, having an ECM area percentage of $6.99 \pm 2.01\%$ (16 FOV) and the PLGA $4.72 \pm 1.56\%$ (16 FOV), respectively, which is significantly different ($p = 0.0012$; Fig. 2f). Concerning cell distribution and cell morphology, histological sections looked very similar for 1 and 2 weeks of cultivation, respectively.

Quantitative analysis of cell proliferation

In order to quantify cell proliferation of ASC, PLGA/a CaP tubes were seeded with 1 million of ASC outside and 1 million of ASC inside and histological paraffin sections were analysed. Only PLGA/a CaP tubes were used (no PLGA tubes), because the comparison of cell attachment and qualitative proliferation of cells on either PLGA or PLGA/a CaP had been made in the experiments using the corresponding electrospun disks and no difference had been determined. As can be seen in Fig. 3a, the cell distribution over the wall of the tubes was similar for all 8 tubes. The tube wall was divided into three sections, one third outside, one third in the middle and one third inside, respectively. Independent of the passage number (P4 versus P7) and also independent of the cultivation time (1 week versus 2 weeks), cells were similarly distributed over the three parts. In all tube specimens, the middle section contained around half the amount of ASC compared to the end sections.

Starting with a total of 2 millions of ASC per tube (time point 0), we found on average 8.4 ± 3.5 millions after 1 week ($n = 4$) and 8.0 ± 0.5 millions after 2 weeks ($n = 4$) (Fig. 3b) after upscaling the findings for the cell number found for the inside, middle and outside sections, respectively. Even with one of the weakest post hoc tests (Fisher's PLSD), no significant difference was found between 1 week and 2 week experiments ($p = 0.79$).

A CaP nanoparticles as a trigger for osteogenesis

To test whether a CaP nanoparticles (without scaffold) trigger the differentiation of ASC towards an osteoblast phenotype, we added 5, 50 and 500 µg mL⁻¹ pure a CaP in DMEM (control: no a CaP, Fig. 4a) to ASC (P5) and analysed for osteocalcin protein expression after 1 and 2 weeks using immunocytochemistry. Untreated human osteoblasts served as positive control (Fig. 4b). Cells that were exposed to 500 µg mL⁻¹ a CaP died after one day. The impact of 5 and 50 µg mL⁻¹ a CaP are shown in Fig. 4c and d, respectively. After 1 week, some ASC cells in the 5 µg mL⁻¹ TCP samples expressed osteocalcin. However, in contrast to the rather big osteoblasts, ASC retained their morphology and size (small). In the 50 µg mL⁻¹ a CaP samples, more cells expressed osteocalcin compared to the 5 µg mL⁻¹ a CaP samples. However, compared to

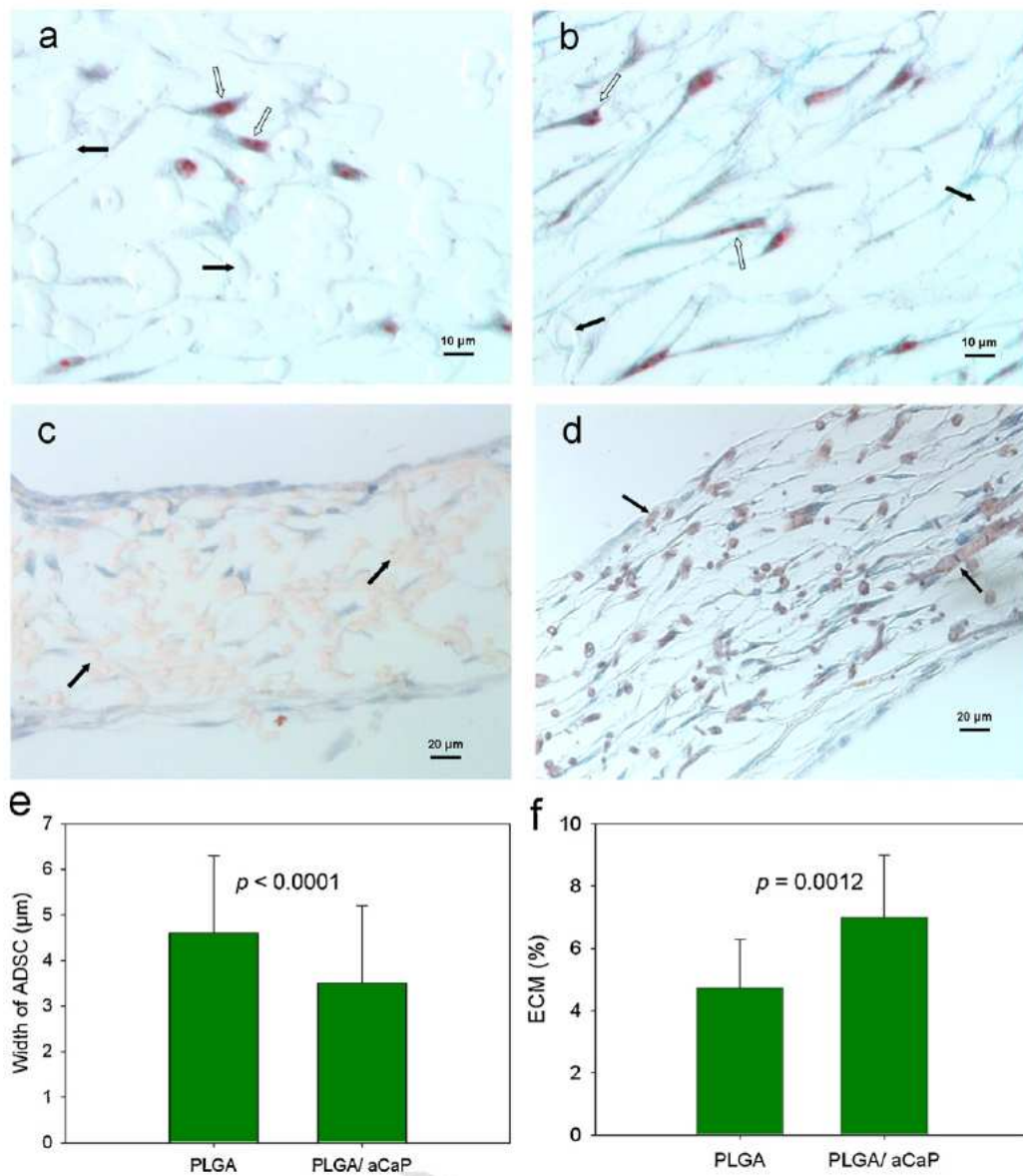


Fig. 2. Masson Goldner Trichrome staining of ASC on PLGA (a) and PLGA/aCaP (b) and Hemalaun/Sudan staining of ASC on PLGA disc (c) and PLGA/aCaP disc (d) after two weeks of cultivation *in vitro*. Black arrows denote the scaffold material. Cells undergoing mitosis are marked with empty arrows in (a) and (b). In PLGA/aCaP the ASC had a spindle-shaped and fibroblast-like morphology whereas in the PLGA they were roundish leading to statistically significantly different widths (e). Extracellular matrix production was significantly higher for the PLGA/aCaP material compared to neat PLGA (f). Independent of the material ASC were evenly distributed.

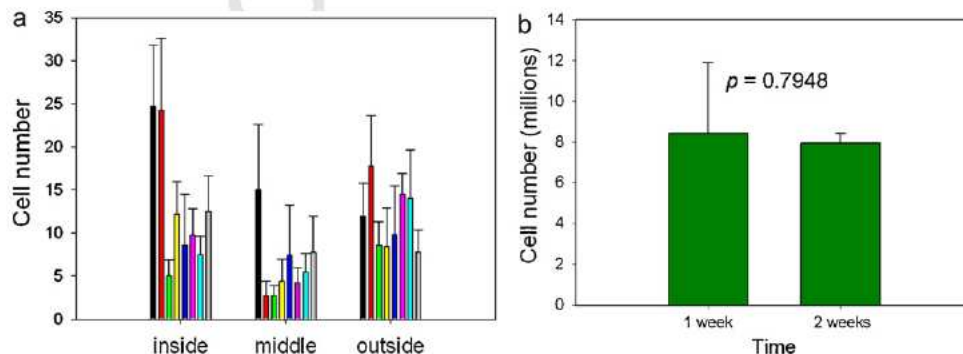


Fig. 3. Distribution of human ASC on electrospun PLGA/aCaP tubes, (a) cell distribution in histological cross-sections of 200 µm based on at least 4 fields of view (FOV) for eight individual tubes in the inside, middle and outside part of the wall with the first four bars denoting 1-week-experiments and the second 4 bars 2-week-experiments, (b) average and standard deviation of total cell number per tube for 1- and 2-week-experiments, respectively ($n = 4$). Error bars denote standard deviation.

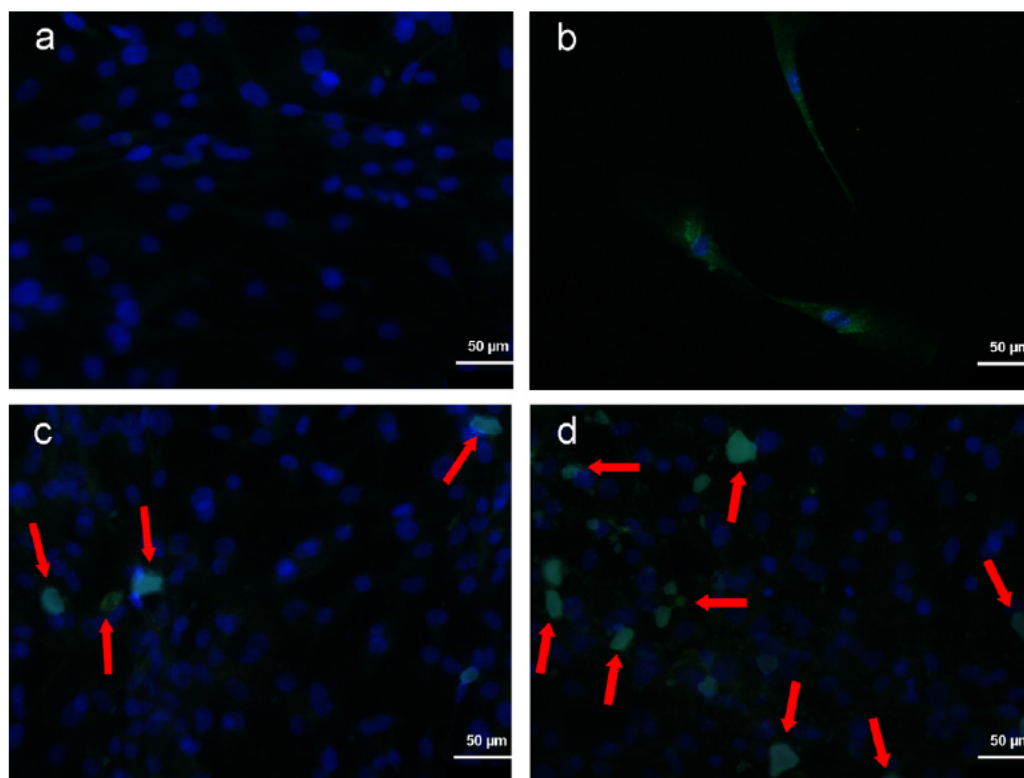


Fig. 4. Immunocytochemical analysis for osteocalcin expression on ASC after 1 week of cultivation in DMEM: (a) human ASC (P5) without a-CaP nanoparticles (negative control), (b) human osteoblasts (positive control), (c) human ASC with 5 $\mu\text{g mL}^{-1}$ a-CaP in DMEM and (d) human ASC with 50 $\mu\text{g mL}^{-1}$ a-CaP in DMEM. Note: the morphology of all ASC remained the same despite of osteocalcin expression in a few cells (green; depicted by red arrows) denoting only a commitment towards osteoblasts, but not a full Q5 differentiation. Results for 2 weeks cultivation were similar. (For interpretation of the references to color in this figure legend, the reader is referred to the web version of the article.)

the 5 $\mu\text{g mL}^{-1}$ a-CaP samples, the cells were found to be a little less dense and some cells were lysed. Results after 2 weeks incubation were similar (data not shown).

Vascularisation

Vascularisation of the PLGA/a-CaP and PLGA (no cell seeding) material was studied by placing the PLGA disks, the PLGA/a-CaP disks and the 0.5 cm electrospun tubes carefully on top of the chorioallantoic membrane (CAM) at ID 8 (Fig. 5a). After one week, the PLGA/a-CaP tubes (Fig. 5b) and the PLGA disks (Fig. 5c) were well penetrated and coated by vessels (paraffin sections). The same was found for the PLGA/a-CaP disks (data not shown). Vessels could clearly be found to be homogeneously distributed over the whole tube wall, as shown in the H&E stained cross section at 25 \times magnification (Fig. 5d) and exemplified for both materials in a Hemalaun Sudan stained section at 400 \times magnification where the roundish vessels contain brownish stained erythrocytes (Fig. 5e and f).

Discussion

In order to repair traumatic and degenerative bone loss or after bone tumour resections, critical size bone grafts are required.^{4,15,25} As a golden standard, autologous bone is grafted at the site of bone loss with many possible disadvantages involved; chronic pain at the harvest site, neurovascular injury, limited availability and insufficient biomechanical properties. These limitations may be overcome by tissue engineered grafts including a biocompatible and biodegradable scaffold material and an osteogenic, vasculogenic and/or stem cell source to form new bone tissue as well as a

pre engineered vascular network enabling rapid anastomosis and perfusion.^{32–34}

In the present study, we tested for the first time the biocompatible properties of a recently developed nanocomposite consisting of PLGA and a CaP nanoparticles (60/40 wt) scaffold² for growth of human ASC from an abdominal fat source. The better bone formation of PLGA/ β TCP with rabbit ASC compared to scaffolds without cells has been reported lately for *in vivo* experiments.¹¹ Therefore, as a first step towards such an ASC seeded bone graft based on PLGA/a-CaP nanocomposite, we evaluated the behaviour of human ASC on electrospun PLGA/a-CaP compared to pure electrospun PLGA. Although electrospun materials do not have the physical strength of bone just right after implantation, such materials seeded with cells can induce bone formation after *in vivo* integration so that the necessary strength will be provided. Our main findings were that the human ASC attached very well on the surface of both materials *in vitro* (without any help of collagen coating as is for example needed for cell attachment on DegraPol^{®13}). Moreover, the ASC showed a homogenous and fast three dimensional ingrowth into the nanocomposite as well as into the reference material PLGA. For both materials, we detected cells in a mitotic stage which confirms their *in situ* proliferation.

a-CaP nanoparticles render the surface of the PLGA fibres rough. Surface properties have been reported to modulate cell activity.^{35,36} When the electrospun PLGA/a-CaP disks were compared with neat PLGA disks, however, we only found differences in the morphology of the ASC after 1 week of cultivation, namely that the ASC on PLGA/a-CaP retained their morphology and size, while the ASC on PLGA got wider and roundish. In contrast, such morphological changes have not been observed in similar

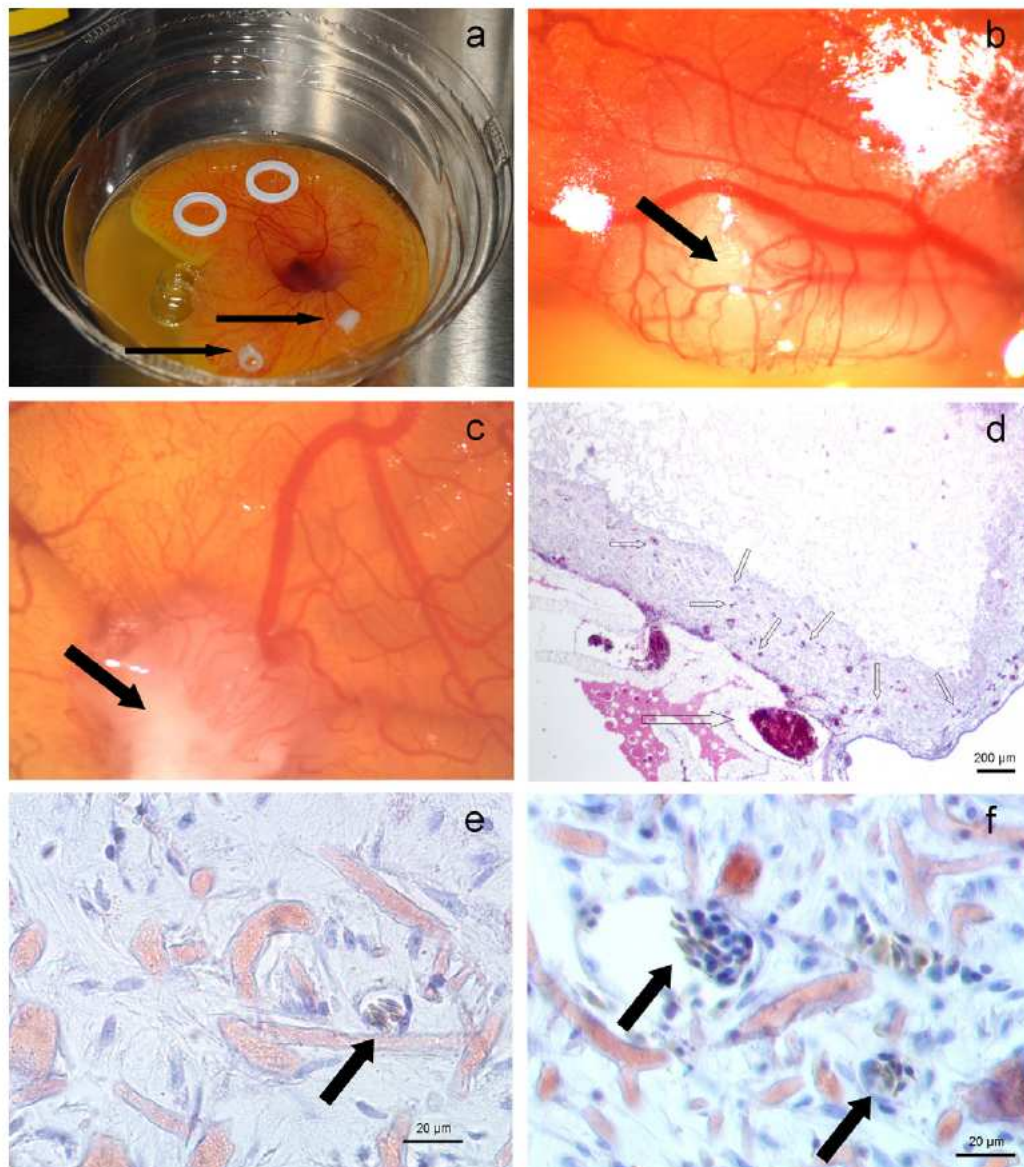


Fig. 5. Vascularisation of the PLGA/a-CaP and PLGA material without cells on the CAM. (a) PLGA/a-CaP tubes at time 0 (ID 8 of the chick embryo; black arrows); (b) tube (black arrow) after 7 days on CAM (ID 15 of the chick embryo); (c) PLGA disc (black arrow) after 7 days on the CAM; (d) histological cross-section of tube wall stained by Haematoxylin–Eosin, selected vessels in the tube wall (small arrows), a big vessel outside the tube (big arrow), the erythrocytes are stained dark red; note that the tube wall has shrunk from 800 µm to 500 µm caused by capillary forces. Hemalaun–Sudan staining showing PLGA/a-CaP (e) and PLGA (f) with fibres in light red, fibroblasts in violet and erythrocytes inside the vessel wall brownish (arrows). (For interpretation of the references to color in this figure legend, the reader is referred to the web version of the article.)

experiments where stem cells originating from bone marrow have been applied.² Moreover, on the PLGA/a CaP scaffold the ECM production was significantly higher compared to pure PLGA. This stands in accordance with the finding of Lv et al. which demonstrates that hydroxylapatite nanoparticles (100 nm) on PLGA promoted proliferation of human mesenchymal stem cells compared to PLGA alone.¹⁰

Based on the fact that ASC did not show differences with respect to attachment and qualitative proliferation on the disks, we chose tubes of PLGA/a CaP for the quantitative evaluation of ASC proliferation. Tubes 2 cm in length with walls of ~800 µm thickness and an inner diameter of 2 mm were used. The idea behind this special scaffold architecture was that ASC seeded inside might build up enough cell layers to contact and connect to cells vis à vis inside the tube, which would make such a bone graft attractive for *in vivo* cylinder shaped bone defects. The inner

diameter of 2 mm, however, was too large to see such a bridging effect within 2 weeks. Doubling times (DT) found for the proliferation of ASC on these PLGA/a CaP tubes were 3.5 days in the first week of cultivation and then the cell number plateaued. For comparison, *in vitro* DT for ASC from rats, rabbits and pigs are 3.5, 1.9 and 2.3 days, respectively.³⁷ Human ASC have DT of 2 days³⁸ to 3 days³⁹ in culture medium. Between day 3 and day 7 (log phase), a doubling time of 2 days to 3 days was also found for ASC of differently aged donors.⁴⁰ Another important point is that proliferation of cells in a 3D scaffold is different from 2D expansion. For example, Cao et al. reported that human MSCs had a smaller initial cell growth rate in 3D scaffolds compared to 2D expansion, however, on 3D scaffolds, the long term culture stability improved.⁴¹ Thus, with an observed DT of 3.5 days on the three dimensional PLGA/a CaP scaffold, cells obviously have a favourable environment to expand. Proliferation into the 800 µm tube wall

clearly plateaued after one week (without any cell debris) although a homogenous distribution over the whole wall was not yet achieved (no saturation as found in the 200 μm disks). The same results were obtained by Haimi et al. They report an increase of ASC number on bioactive glass composites in the first week and then no change in cell number in the subsequent week of cultivation.⁴² It is probable that further space for proliferation was getting limited and/or that osteogenic differentiation process had started, which might slow down cell proliferation as described for other cells.⁴³

It has been reported that a pure α TCP porous scaffold seeded with ASC triggers their differentiation into osteoblasts in the absence of osteogenic supplements.⁴⁴ As β TCP is a rather brittle material with low mechanical strength and therefore not optimal for bone reconstruction, it would be desirable to have the same differentiation impact triggered by amorphous (nano) particles because such particles could be combined with any other synthetic polymer to guarantee sufficient biomechanical properties⁴⁵ and they are more reactive compared to α TCP.⁴⁶ We therefore incubated ASC with different concentrations of a CaP nanoparticles in normal cultivation medium and measured expression of osteocalcin by immunocytochemistry. At 500 $\mu\text{g mL}^{-1}$, all cells died the day after. Obviously, the concentration was too high and toxic. Cells normally tolerate concentrations of up to 200 $\mu\text{g mL}^{-1}$, which has been demonstrated for lung fibroblasts exposed to nano haematite (70 nm) and silicate (40 nm)⁴⁷ or to ceria oxide nanoparticles.⁴⁸ Exposed to 5 and 50 $\mu\text{g mL}^{-1}$ a CaP, however, ASC expanded well and showed some osteocalcin expression after 1 week (similar results after 2 weeks). The morphology of the ASC, however, was still ASC like and not osteoblast like; indicating a hybrid cell type committed towards the osteoblast phenotype. We conclude from these observations that a CaP nanoparticles suspended at low concentrations in normal culture medium trigger the differentiation of human ASC towards a phenotype committed to osteogenesis, which dexamethasone for osteoblast differentiation unnecessary.²⁸ Whether the differentiation process is triggered by mere contact of ASC with a CaP nanoparticles on the surface of the cells or whether the particles must be taken up by the cells will be the focus of further investigation in our laboratories.

Insufficient vascularisation leading to a necrotic core in the bone graft is still the bottleneck in tissue engineering of bone constructs up to date.^{4,18} Approaches with preformed capillaries either provoked *in situ*,²⁰ by cell seeding of co cultures with a vasculogenic cell type,¹⁶ or by dynamic seeding with (oscillatory) perfusion techniques⁴⁹ have been shown to improve the situation after implantation. In the present study, we investigated whether the electrospun PLGA/a CaP scaffold material would be easily penetrated by invasion of avian vessels from the chorioallantoic membrane of a chick embryo *in vivo*. After 1 week, we found a homogenous vascularisation outside and inside the vessel wall. Obviously, the pore size and the material properties are favourable for vessel ingrowth. PLGA/a CaP performed at least as good as PLGA with respect to vascularisation, which implies that the a CaP nanoparticles do not hinder vessel ingrowth. This suggests the suitability of an electrospun PLGA/a CaP scaffold material as an effective scaffold for tissue engineering of bone grafts.

As a summary, we found that the combination of an electrospun PLGA/a CaP nanocomposite with human ASC was suitable for tissue engineering of bone constructs because cells attached and proliferated very well on this scaffold material. Moreover, a CaP nanoparticles applied in low concentrations triggered osteocalcin expression in human ASC, which makes them *per se* an interesting and potential partner for synthesizing nanocomposites with any other polymer instead of PLGA. Finally, the electrospun PLGA/a CaP nanocomposite has an excellent architecture with respect to vessel ingrowth as shown by a full and homogenous vascularisation of a $\sim 800 \mu\text{m}$ thick layer within 1 week.

Conflict of interest statement

No potential financial or personal conflicts exist.
This work is not being submitted elsewhere for publication.

Acknowledgements

We thank Miss Gabriella Meier Bürgisser for measuring the widths of the ASC in the histological cross sections. Miss Pia Fuchs is acknowledged for help with histological staining.

Appendix A. Supplementary data

Supplementary data associated with this article can be found, in the online version, at <http://dx.doi.org/10.1016/j.injury.2012.06.004>.

References

- Hild N, Schneider OD, Mohn D, Luechinger NA, Koehler FM, Hofmann S, et al. Two-layer membranes of calcium phosphate/collagen/PLGA nanofibres: in vitro Q3 biomineralisation and osteogenic differentiation of human mesenchymal stem cells. *Nanoscale* 2011;3(2):401–9.
- Schneider OD, Lohrer S, Brunner TJ, Uebersax L, Simonet M, Grass RN, et al. Cotton wool-like nanocomposite biomaterials prepared by electrospinning: in vitro bioactivity and osteogenic differentiation of human mesenchymal stem cells. *Journal of Biomedical Materials Research Part B Applied Biomaterials* 2008;84B(2):350–62.
- Lohrer S, Reboul V, Brunner TJ, Simonet M, Dora C, Neuenschwander P, et al. Improved degradation and bioactivity of amorphous aerosol derived tricalcium phosphate nanoparticles in poly(lactide-co-glycolide). *Nanotechnology* 2006;17(8):2054–61.
- Scherberich A, Muller AM, Schafer DJ, Banfi A, Martin I. Adipose tissue-derived progenitors for engineering osteogenic and vasculogenic grafts. *Journal of Cellular Physiology* 2010;225(2):348–53.
- Shapiro F. Bone development and its relation to fracture repair. The role of mesenchymal osteoblasts and surface osteoblasts. *European Cells & Materials* 2008;1553–76.
- Rucker M, Laschke MW, Junker D, Carvalho C, Tavassol F, Mulhaupt R, et al. Vascularization and biocompatibility of scaffolds consisting of different calcium phosphate compounds. *Journal of Biomedical Materials Research Part A* 2008;86A(4):1002–11.
- Alcaide M, Serrano MC, Pagani R, Sanchez-Salcedo S, Vallet-Regi M, Portoles MT. Biocompatibility markers for the study of interactions between osteoblasts and composite biomaterials. *Biomaterials* 2009;30(1):45–51.
- Liu QH, Cen L, Yin S, Chen L, Liu GP, Chang J, et al. A comparative study of proliferation and osteogenic differentiation of adipose-derived stem cells on akermanite and beta-TCP ceramics. *Biomaterials* 2008;29(36):4792–9.
- Du DJ, Furukawa K, Ushida T. Oscillatory perfusion seeding and culturing of osteoblast-like cells on porous beta-tricalcium phosphate scaffolds. *Journal of Biomedical Materials Research Part A* 2008;86A(3):796–803.
- Lv Q, Nair L, Laurencin CT. Fabrication, characterization, and in vitro evaluation of poly(lactic acid glycolic acid)/nano-hydroxyapatite composite microsphere-based scaffolds for bone tissue engineering in rotating bioreactors. *Journal of Biomedical Materials Research Part A* 2009;91A(3):679–91.
- Hao W, Pang L, Jiang M, Lv R, Xiong Z, Hu YY. Skeletal repair in rabbits using a novel biomimetic composite based on adipose-derived stem cells encapsulated in collagen I gel with PLGA-beta-TCP scaffold. *Journal of Orthopaedic Research* 2010;28(2):252–7.
- Bernhardt A, Lode A, Boxberger S, Pompe W, Gelinsky M. Mineralised collagen – an artificial, extracellular bone matrix – improves osteogenic differentiation of bone marrow stromal cells. *Journal of Materials Science: Materials in Medicine* 2008;19(1):269–75.
- Buschmann J, Welti M, Hemmi S, Neuenschwander P, Baltes C, Rudin M, et al. 3D co-cultures of osteoblasts and endothelial cells in DegraPol foam: histological and high field MRI analyses of pre-engineered capillary networks in bone grafts. *Tissue Engineering Part A* 2011;17(3–4):291–9.
- Stiehler M, Bunker C, Baatrup A, Lind M, Kassem M, Mygind T. Effect of dynamic 3-D culture on proliferation, distribution, and osteogenic differentiation of human mesenchymal stem cells. *Journal of Biomedical Materials Research Part A* 2009;89A(1):96–107.
- Santos MI, Reis RL. Vascularization in bone tissue engineering: physiology, current strategies, major hurdles and future challenges. *Macromolecular Bioscience* 2010;10(1):12–27.
- Fuchs S, Jiang X, Schmidt H, Dohle E, Ghanaati S, Orth C, et al. Dynamic processes involved in the pre-vascularization of silk fibroin constructs for bone regeneration using outgrowth endothelial cells. *Biomaterials* 2009;30(7):1329–38.
- Yu HY, VandeVord PJ, Mao L, Matthew HW, Wooley PH, Yang SY. Improved tissue-engineered bone regeneration by endothelial cell mediated vascularization. *Biomaterials* 2009;30(4):508–17.

- Q4 18. Laschke MW, et al. Angiogenesis in tissue engineering: breathing life into constructed tissue substitutes. *Tissue Engineering* 2006;12(8):2093–104.
19. Steffens L, Wenger A, Stark GB, Finkenzeller G. In vivo engineering of a human vasculature for bone tissue engineering applications. *Journal of Cellular and Molecular Medicine* 2009;13(9B):3380–6.
20. Laschke MW, Rucker M, Jensen G, Carvalho C, Mulhaupt R, Gellrich NC, et al. Improvement of vascularization of PLGA scaffolds by inoculation of in situ-preformed functional blood vessels with the host microvasculature. *15th annual meeting of the European Surgical Association*. Venice, ITALY: Lippincott Williams & Wilkins; 2007.
21. Manasseri B, et al. Microsurgical arteriovenous loops and biological templates: a novel in vivo chamber for tissue engineering. *Microsurgery* 2007;27(7):623–9.
22. Muller AM, Mehrkens A, Schafer DJ, Jaquiere C, Guven S, Lehmicke M, et al. Towards an intraoperative engineering of osteogenic and vasculogenic grafts from the stromal vascular fraction of human adipose tissue. *European Cells & Materials* 2010;19(1):127–35.
23. Schneider OD, Weber F, Brunner TJ, Loher S, Ehrbar M, Schmidlin PR, et al. In vivo and in vitro evaluation of flexible, cottonwool-like nanocomposites as bone substitute material for complex defects. *Acta Biomaterialia* 2009;5(5):1775–84.
24. Schneider OD, Mohn D, Fuhrer R, Klein K, Kämpf K, Nuss KMR, et al. Biocompatibility and bone formation of flexible, cotton wool-like PLGA/calcium phosphate nanocomposites in sheep. *The Open Orthopaedics Journal* 2011;5(1):57–65.
25. Tapp H, Hanley EN, Patt JC, Gruber HE. Adipose-derived stem cells: characterization and current application in orthopaedic tissue repair. *Experimental Biology and Medicine* 2009;234(1):1–9.
26. Zuk PA, Zhu M, Ashjian P, De Ugarte DA, Huang JL, Mizuno H, et al. Human adipose tissue is a source of multipotent stem cells. *Molecular Biology of the Cell* 2002;13(12):4279–95.
27. Loher S, Stark WJ, Maciejewski M, Baiker A, Pratsinis SE, Reichardt D, et al. Fluoro-apatite and calcium phosphate nanoparticles by flame synthesis. *Chemistry of Materials* 2005;17(1):36–42.
28. Zuk PA, Zhu M, Mizuno H, Huang J, Futrell JW, Katz AJ, et al. Multilineage cells from human adipose tissue: implications for cell-based therapies. *Tissue Engineering* 2001;7(2):211–28.
29. Fraser JK, Wulur I, Alfonso Z, Hedrick MH. Fat tissue: an under appreciated source of stem cells for biotechnology. *Trends in Biotechnology* 2006;24(4):150–4.
30. Gronthos S, Franklin DM, Leddy HA, Robey PG, Storms RW, Gimble JM. Surface protein characterization of human adipose tissue-derived stromal cells. *Journal of Cellular Physiology* 2001;189(1):54–63.
31. Trentz OA, Hoerstrup SP, Sun LK, Bestmann L, Platz A, Trentz OL. Osteoblasts response to allogenic and xenogenic solvent dehydrated cancellous bone in vitro. *Biomaterials* 2003;24(20):3417–26.
32. Dyson JA, Genever PG, Dalgarno KW, Wood DJ. Development of custom-built bone scaffolds using mesenchymal stem cells and apatite–wollastonite glass-ceramics. *Tissue Engineering* 2007;13(12):2891–901.
33. Cancedda R, Giannoni P, Mastrogiacomo M. A tissue engineering approach to bone repair in large animal models and in clinical practice. *Biomaterials* 2007;28(29):4240–50.
34. Tortelli F, Pujic N, Liu Y, Laroche N, Vico L, Cancedda R. Osteoblast and osteoclast differentiation in an in vitro three-dimensional model of bone. *Tissue Engineering Part A* 2009;15(9):2373–83.
35. Boyan BD, Hummert TW, Dean DD, Schwartz Z. Role of material surfaces in regulating bone and cartilage cell response. *Biomaterials* 1996;17(2):137–46.
36. Kieswetter K, Schwartz Z, Hummert TW, Cochran DL, Simpson J, Dean DD, et al. Surface roughness modulates the local production of growth factors and cytokines by osteoblast-like MG-63 cells. *Journal of Biomedical Materials Research* 1996;32(1):55–63.
37. Arrigoni E, Lopa S, de Girolamo L, Stanco D, Brini AT. Isolation, characterization and osteogenic differentiation of adipose-derived stem cells: from small to large animal models. *Cell and Tissue Research* 2009;338(3):401–11.
38. Pautke C. *Charakterisierung von humanen mesenchymalen Stammzellen und Zellen der osteoblastären Differenzierungskaskade*. Munich: Universität München; 2004.
39. Bertram H. *Untersuchung zur Osteogenese von humanen mesenchymalen Stammzellen*. Braunschweig: Technical University of Carolo-Wilhelmina; 2002.
40. Zhu M, Kohan E, Bradley J, Hedrick M, Benhaim P, Zuk PA. The effect of age on osteogenic, adipogenic and proliferative potential of female adipose-derived stem cells. *Journal of Tissue Engineering and Regenerative Medicine* 2009.
41. Cao Y, Li D, Shang C, Yang S-T, Wang J, Wang X. Three-dimensional culture of human mesenchymal stem cells in a polyethylene terephthalate matrix. *Bio-medical Materials* 2010;5:065013.
42. Haimi S, Suuriniemi N, Haaparanta AM, Ella V, Lindroos B, Huhtala H, et al. Growth and osteogenic differentiation of adipose stem cells on PLA/bioactive glass and PLA/beta-TCP scaffolds. *Tissue Engineering Part A* 2009;15(7):1473–80.
43. Miller JP, Yeh N, Vidal A, Koff A. Interweaving the cell cycle machinery with cell differentiation. *Cell Cycle* 2007;6(23):2932–8.
44. Marino G, Rosso F, Cafiero G, Tortora C, Moraci M, Barbarisi M, et al. beta-Tricalcium phosphate 3D scaffold promote alone osteogenic differentiation of human adipose stem cells: in vitro study. *Journal of Materials Science Materials in Medicine* 2010;21(1):353–63.
45. Mohn D, Ege D, Feldman K, Schneider OD, Imfeld T, Boccaccini AR, et al. Spherical calcium phosphate nanoparticle fillers allow polymer processing of bone fixation devices with high bioactivity. *Polymer Engineering and Science* 2010;50(5):952–60.
46. Brunner TJ, Bohner M, Dora C, Gerber C, Stark WJ. Comparison of amorphous TCP nanoparticles to micron-sized alpha-TCP as starting materials for calcium phosphate cements. *Journal of Biomedical Materials Research Part B Applied Biomaterials* 2007;83B(2):400–7.
47. Wottrich R. Toxicological studies of ultrafine particles: development and application of a close-to-reality in vitro lung model. *Institute for Toxicology*. Karlsruhe: University of Karlsruhe; 2003. p. 125.
48. Limbach LK, Li YC, Grass RN, Brunner TJ, Hintermann MA, Muller M, et al. Oxide nanoparticle uptake in human lung fibroblasts: effects of particle size, agglomeration, and diffusion at low concentrations. *Environmental Science & Technology* 2005;39(23):9370–6.
49. Du DJ, Furukawa KS, Ushida T. 3D culture of osteoblast-like cells by unidirectional or oscillatory flow for bone tissue engineering. *Biotechnology and Bioengineering* 2009;102(6):1670–8.